INFECTION AND IMMUNITY, Apr. 2007, p. 1626–1634 Vol. 75, No. 4
0019-9567/07/$08.00+0 doi:10.1128/IAI.01862-06

Bradyzoite-Specific Surface Antigen SRS9 Plays a Role in Maintaining *Toxoplasma gondii* Persistence in the Brain and in Host Control of Parasite Replication in the Intestine[▽]

Seon-Kyeong Kim, Ariela Karasov,† and John C. Boothroyd*

Department of Microbiology and Immunology, Stanford University School of Medicine, 299 Campus Dr., Stanford, California 94305

Received 26 November 2006/Returned for modification 5 January 2007/Accepted 21 January 2007

Toxoplasma gondii **is a ubiquitous parasite that persists for the life of a healthy mammalian host. A latent, chronic infection can reactivate upon immunosuppression and cause life-threatening diseases, such as encephalitis. A key to the pathogenesis is the parasite's interconversion between the tachyzoite (in acute infection) and bradyzoite (in chronic infection) stages. This developmental switch is marked by differential expression of numerous, closely related surface proteins belonging to the SRS (*S*AG1-*r*elated *s*equence) superfamily. To probe the functions of bradyzoite-specific SRSs, we created a bioluminescent strain lacking the expression of SRS9, one of the most abundant SRSs of the bradyzoite stage. Imaging of mice intraperitoneally infected with tachyzoites revealed that during an acute infection, wild-type and Δ*srs9* strains replicated at similar rates, disseminated systemically following similar kinetics, and initially yielded similar brain cyst numbers. However, during a chronic infection, Δ*srs9* cyst loads substantially decreased compared to those of the wild type, suggesting that SRS9 plays a role in maintaining parasite persistence in the brain. In oral infection with bradyzoite cysts, the Δ*srs9* strain showed oral infectivity and dissemination patterns indistinguishable from those of the wild type. When chronically infected mice were treated with the immunosuppressant dexamethasone, however, the Δ*srs9* strain reactivated in the intestinal tissue after only 8 to 9 days, versus 2 weeks for the wild-type strain. Thus, SRS9 appears to play an important role in both persistence in the brain and reactivation in the intestine. Possible mechanisms for this are discussed.**

Toxoplasma gondii is an intracellular protozoan parasite that can infect a wide range of mammalian hosts. The parasite switches between two different developmental forms in its intermediate hosts: the tachyzoite, which rapidly divides and disseminates during an acute infection; and the bradyzoite, which encysts and persists in tissues. One hallmark of the *Toxoplasma* developmental switch is the differential expression of numerous, closely related glycophosphatidylinositol-anchored surface proteins belonging to the SRS (*S*AG1-*r*elated *s*equence) superfamily (>160 putative genes) (10). Nucleotide sequence identity can be 20 to 90%, depending on subfamilies. SAG1, the most abundant SRS antigen, is specific to the tachyzoite stage and serves as a prototype (22). The majority of SRS antigen genes are ~1.5 kb in length, lack introns, and are found scattered throughout the genome in tandemly arrayed multigenic clusters with intergenic distances ranging typically from 1.5 to 2.5 kb (10). The transcription start site is in the same orientation for every gene within a cluster, indicating that these clusters have probably arisen through gene duplication. For the majority of SRS sequences for which multiple expressed sequence tags exist, mRNA expression is developmentally regulated such that tachyzoites and bradyzoites express largely nonoverlapping sets of multiple SRS genes (10).

The purposes served by the SRS antigens may be diverse. SRS antigens are thought to facilitate attachment to and invasion of a host cell (6, 9, 13, 18), but the identity of the interacting host cell ligands remains elusive. Recently, X-ray crystallography has revealed that the highly abundant SAG1 specific to the tachyzoite stage forms a homodimer in which the dimeric interface shaped by an extended β-sheet forms a deep groove lined with positively charged amino acids (7). This groove appears likely to be conserved among SRS proteins and potentially serves as a sulfated proteoglycan-binding site on the target cell surface, providing an explanation for how *Toxoplasma* can infect various cell types in a wide range of host species.

In addition to serving as cell adhesion molecules, SRS antigens are important targets of an adaptive immune response. Remarkably, two tachyzoite-specific SRS antigens, SAG1 and SAG2A, have been shown to dominate the serum immunoglobulin G (IgG) response before antibody responses to other tachyzoite antigens can be detected (2, 15). In the C57BL/6 mouse, wild-type (WT) *Toxoplasma* strains cause pathological immune responses in the intestine, but a parasite having a targeted deletion of the *SAG1* gene does not, suggesting that SAG1 plays a critical role in driving a proinflammatory response (16). Via unknown mechanisms, SAG1 protein triggers CCL2 secretion by cultured human fibroblasts (3), a possible mechanism by which cellular infiltrates accumulate at the site of infection causing a pathological inflammation. Recently, we have investigated biological implications of the stage specificity of SRS antigens and have shown that a *SAG1*^{c} mutant that constitutively expresses the normally tachyzoite-specific SAG1

* Corresponding author. Mailing address: Department of Microbiology and Immunology, Stanford University School of Medicine, 299 Campus Dr., Stanford, CA 94305. Phone: (650) 723-7983. Fax: (650) 723-6853. E-mail: jboothr@stanford.edu.

† Present address: University of Wisconsin School of Medicine and Public Health, 750 Highland Ave., Madison, WI 53705-2221.

▽ Published ahead of print on 29 January 2007.

in both tachyzoite and bradyzoite stages elicits a hyperactive T-cell response associated with an overproduction of gamma interferon, tumor necrosis factor alpha, and interleukin-10 (11). Mice infected with the *SAG1*^{c} mutant showed excessive parasite growth in the brain, severe encephalitis, and increased mortality during the chronic phase of infection (11). Thus, it appears that *Toxoplasma* may have evolved to express SAG1 in a tachyzoite-specific manner in order to facilitate parasite persistence by avoiding detrimental consequences to the host.

Most previous work on the SRS biology has been focused on SRS antigens specific to the tachyzoite stage, although one of the major routes of natural infection is a consumption of undercooked meat contaminated with cysts harboring bradyzoites, which are the orally infective forms of the parasite (21). In oral infection with tissue cysts, SRS antigens specific to the bradyzoite stage would be among the first parasite antigens to interact with the intestinal epithelium. However, whether these SRS antigens are indeed key to the attachment to and invasion of intestinal epithelial cells has not previously been determined. In addition, SRS antigens expressed by bradyzoites would also be among the first parasite antigens to be presented to the immune system following ingestion of tissue cysts. However, a number of questions remain unanswered as to the immunogenicity of bradyzoite-specific SRS antigens. Mice and rats infected by oral gavage (20 bradyzoite cysts) or intraperitoneally (up to 4,000 tachyzoites), as well as naturally infected humans (many of whom likely acquired infection by ingestion of tissue cysts) lack detectable immune responses to bradyzoite-specific SRS antigens, such as SRS9, at both acute and chronic stages of the infection (11). It is not entirely clear why bradyzoite SRS antigens are not immunogenic in natural infection despite the fact that these antigens are highly immunogenic in animals if given with an appropriate adjuvant (11). A low number of bradyzoite cysts orally consumed by the hosts and/or a low number of cysts present in tissues during a chronic infection may be one of the possible explanations.

In the present study, we carried out an oral infection of mice with a high dose of bradyzoite cysts to investigate the role of bradyzoite-specific SRS antigens in establishing an infection in the intestine and brain, as well as the nature of host responses they activate. A bioluminescent strain lacking the *SRS9* gene as a result of a targeted deletion facilitated comparative studies with a wild-type strain by live animal imaging.

MATERIALS AND METHODS

***Toxoplasma* culture.** All *Toxoplasma gondii* strains used in this work were derived from the type II Prugniaud (Pru) strain, which lacks the *HPT* (hypoxanthine-xanthine-guanine-phosphoribosyltransferase) gene (PruΔ*hpt*; a kind gift from D. Soldati, University of Geneva, Geneva, Switzerland) (5). Parasites were cultured in Dulbecco's modified Eagle's medium supplemented with 10% fetal calf serum, penicillin (100 U/ml), streptomycin (100 μg/ml), and L-glutamine (2 mM) (GIBCO BRL) in a humidified incubator at 37°C and with 5% CO_2 and maintained by passage in confluent monolayers of human foreskin fibroblasts.

Generation of the GFP- and FLUC-expressing PruΔ*hpt* parasite. The plasmid construct used to engineer the PruΔ*hpt* strain expressing green fluorescent protein (GFP) and firefly luciferase (FLUC) (Fig. 1A) is the same as the pDHFR-Luc-GFP plasmid described in reference 19, except for the use of *GRA2* and *TUB1* promoters to drive the constitutive expression of GFP and FLUC, respectively, in both tachyzoite and bradyzoite stages. The minimal *GRA2* promoter (317 bp) (12) was PCR cloned from the Pru strain genomic DNA using the following primers: 5′-GACCAAGCTTCCCGTCGCACGGTGATACTG-3′ and 5′-CGGCATGCATTGTGAGGCGATATGTGGAGAA-3′. The *FLUC* gene was flanked by the *TUB1* promoter and 3′ downstream sequence of *TUB1* (GenBank accession no. M20024) (kindly provided by G. Arrizabalaga, University of Idaho, Moscow). The resulting pGRA2-GFP/pTUB1-FLUC plasmid was linearized with NotI, and 50 μg of DNA was used to transform 10^7 PruΔ*hpt* tachyzoites by standard electroporation methods (20). Parasites were added to confluent monolayers of human foreskin fibroblasts in 96-well plates (10^4 tachyzoites per well) and grown without drug selection. Almost two-thirds of the wells in all 96-well plates had various numbers of GFP$^+$ parasites after 3 days of culture. Several wells that appeared to be significantly enriched for GFP$^+$ parasites were chosen for expansion. Parasites stably expressing GFP were sorted by fluorescence-activated cell sorting and cloned by limiting dilution. The FLUC activity of each clone was determined by bioluminescence imaging (BLI) of in vitro tachyzoites (see below).

Generation of the bioluminescent Δ*srs9* strain. The Δ*srs9* strain lacking the entire protein-coding region was created from the PruΔ*hpt*/GFP/FLUC strain by deletional mutagenesis. This was achieved by double-homologous recombination with the pMini-HPT knockout vector (kindly provided by D. S. Roos, University of Pennsylvania, Philadelphia) in which the 2.2-kb upstream sequence and 3-kb downstream sequence of the *SRS9* gene were placed flanking the *HPT*-selectable marker (Fig. 1B). The primers used to PCR clone the flanking sequences from the Pru strain genomic DNA are 5′-GGGCGCGGCCGCCGTGACGGGGTTCATTGTTAGT-3′ and 5′-GCGCTCTAGAACGGTTCCTTGAGTTGTTGAAGA-3′ for the 5′ flank and 5′-GGGCAAGCTTCTGAACGCAGAATTCCGTGCTT-3′ and 5′-GCGCCTCGAGCTCCAGTAGCTCCAAGCTCCA-3′ for the 3′ flank.

The *SRS9* knockout construct was linearized with NotI, and 50 μg of DNA was used to transform by electroporation 10^7 PruΔ*hpt*/GFP/FLUC parasites that had been cultured overnight in a high-pH medium (pH 8.1) to induce a conversion to bradyzoites. A stable population was obtained after selection for HPT activity in medium containing mycophenolic acid (100 μg/ml) and xanthine (50 μg/ml), from which clones were derived. Clones were screened by PCR using primer sets designed to detect homologous recombination at both sides of the *SRS9* gene and the lack of the gene itself (data not shown). Clones that resulted from a heterologous insertion of the knockout vector were also obtained and used as a wild-type control in animal studies.

The lack of SRS9 protein expression by Δ*srs9* bradyzoites was confirmed using brain cysts obtained from chronically infected CBA/J mice in immunofluorescence assays using rabbit anti-SRS9 antisera as previously described (11).

Mouse infection and reactivation. Eight-week-old BALB/c or CBA/J female mice were purchased from the Jackson Laboratories. For intraperitoneal (i.p.) infection, mice were injected with 500 tachyzoites prepared in 0.2 ml sterile phosphate-buffered saline (PBS) as described previously (11). For oral infection with bradyzoite cysts, CBA/J mice were infected i.p. with 500 tachyzoites and brain homogenates were prepared at 4 weeks postinfection (p.i.) as described previously (11). GFP$^+$ cysts were counted using an inverted fluorescence microscope, and brain homogenates were adjusted in volume to yield 300 cysts per 0.3 ml of sterile PBS. After overnight starvation, each BALB/c mouse was left alone for 3 h to consume a piece of normal diet on which homogenates containing 300 cysts were placed.

To reactivate a chronic infection, an immunosuppressant drug, dexamethasone (DXM; dexamethasone 21-phosphate disodium salt [Sigma]) was added to drinking water (30 mg/liter) beginning at 8 weeks p.i. (4). Drinking water was replaced every other day with water containing freshly dissolved DXM.

All animal studies have been reviewed and approved by Stanford University's Administrative Panel for Laboratory Animal Care.

BLI. The BLI procedure using the Xenogen IVIS100 charge-coupled device system (Xenogen, Alameda, CA) has been described elsewhere in detail (8, 19). Briefly, to measure FLUC activity in parasite clones or in tissues, serial dilutions of extracellular tachyzoites or tissue homogenates were placed in black 96-well plates (Costar, Corning, NY) and incubated for 10 min at 37°C with the D-luciferin potassium salt substrate (0.15 mg/ml; Xenogen) prior to imaging for 5 min (19). To obtain images of live mice infected with bioluminescent *Toxoplasma* strains, mice were injected i.p. with 0.2 ml of luciferin prepared in sterile PBS (150 mg substrate/kg body weight) and anesthetized with isoflurane. Imaging was started 10 min after the substrate was given. All mice were imaged ventrally and then dorsally, 5 min each side. Flux was calculated in regions of interest using the Living Image software (Xenogen) and Igor (WaveMetricx, Lake Oswego, OR).

Assessment of brain cyst loads and cyst size. Chronically infected CBA/J mice were sacrificed at indicated time points after i.p. infection with 500 tachyzoites, and brain homogenates were prepared as described previously (11). GFP$^+$ cysts were counted in 20% of the whole brain. Cyst diameter was measured in photographs of hematoxylin- and eosin-stained brain sections taken with a camera

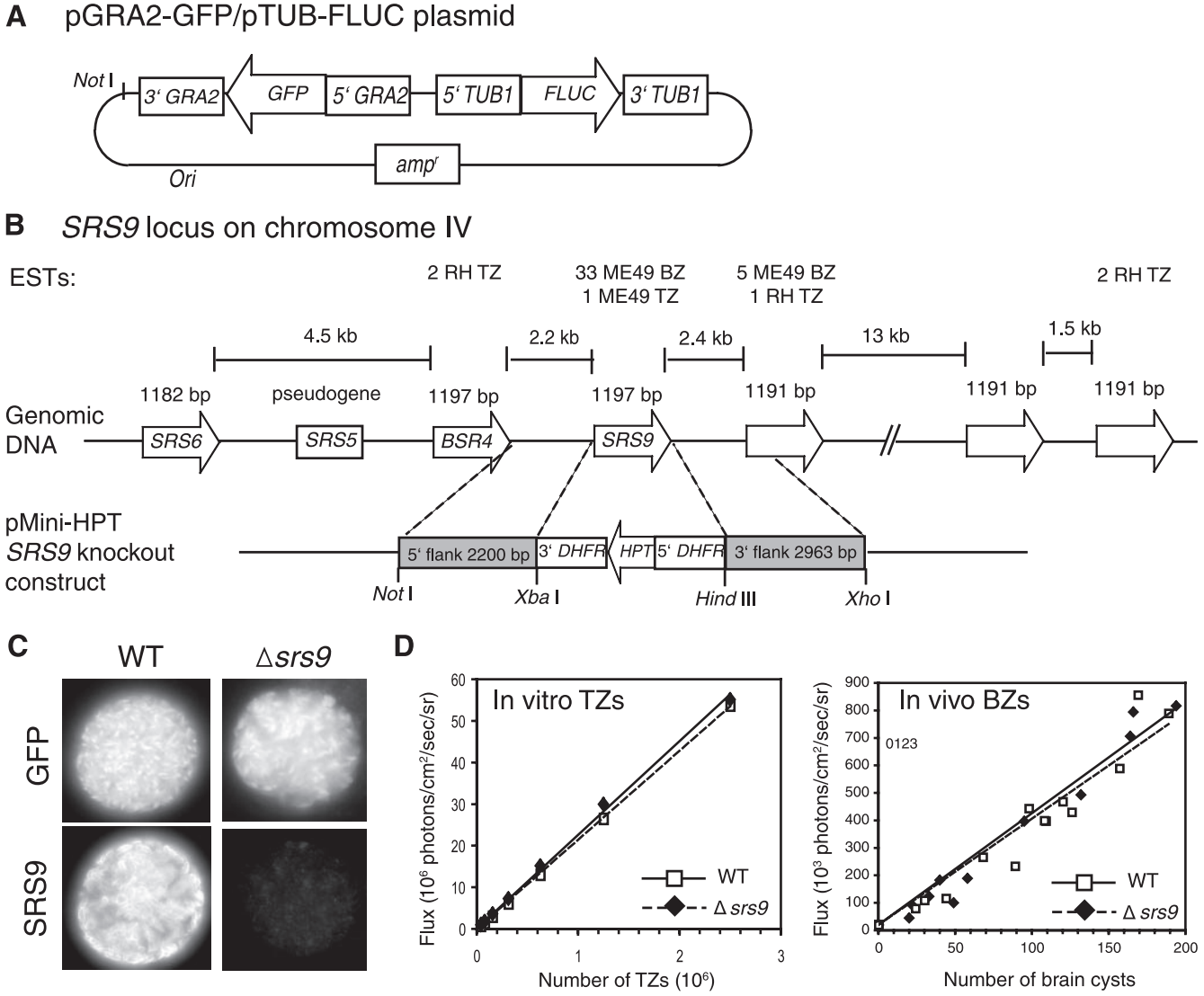

FIG. 1. Generation of a bioluminescent *Toxoplasma* PruΔ*srs9* strain. (A) Depiction of the pGRA2-GFP/pTUB1-FLUC plasmid used to create the bioluminescent PruΔ*hpt* strain without using any drug selection. The map is not drawn to scale. (B) Depiction of the *SRS9* locus on *Toxoplasma* chromosome IV. Six closely related, intron-free genes and one pseudogene are tandemly located as a cluster. The map is not drawn to scale. The number of expressed sequence tags (ESTs) known for each gene is shown (http://www.toxodb.org/toxo-release4-0/home.jsp). Double-homologous recombination between the *SRS9* knockout construct and genomic sequence replaces *SRS9* with *HPT*, which was used for positive selection. TZ, tachyzoites. (C) Immunofluorescence assays confirming the lack of SRS9 protein expression by Δ*srs9* parasites derived from the PruΔ*hpt*/GFP/FLUC strain. Brain cysts from chronically infected CBA/J mice were stained with a rabbit polyclonal anti-SRS9 antiserum. (D) FLUC activity comparison between WT and Δ*srs9* strains. Various numbers of tachyzoites released from human fibroblasts in culture were plated in a black 96-well plate (twofold serial dilutions starting from 2×10^6 tachyzoites), and photon flux was detected by using the IVIS100 imaging system. For bradyzoites (BZ), brain homogenates from WT- or Δ*srs9* parasite-infected CBA/J mice (6 weeks after i.p. infection with 500 tachyzoites) were plated in a black 96-well plate. GFP^+ cysts were counted in each well, and photon flux was determined by BLI after addition of luciferin. There is no significant difference in brain cyst sizes between WT and Δ*srs9* strains (see Fig. 3B). Photon flux from tachyzoites and brain cysts from a parasite strain lacking the *FLUC* gene was equal to that of culture medium alone (data not shown). Lines within graphs represent linear regression correlation.

attached to a microscope as described previously (11) and presented as an arbitrary scale.

Plaque assays. Human foreskin fibroblasts and rat astrocytes (kindly provided by B. Barres, Stanford University, Stanford, CA) were grown to confluence in 12-well plates. GFP^+ cysts were counted in brain homogenates prepared from chronically infected CBA/J mice. Homogenates containing 10 cysts were resuspended in 0.5 ml PBS and syringe lysed to release bradyzoites using a 27-gauge needle followed by a 30-gauge needle. Homogenate volumes equivalent to 1, 2, or 4 cysts were added to host cells in triplicate and cultured for 5 days. Plaques were identified and counted by fluorescence light microscopy using parasite GFP to facilitate identification. A single cyst is thought to contain from hundreds up to a few thousand bradyzoites. WT and Δ*srs9* strains showed similar brain cyst sizes (see Results): tachyzoites maintained in tissue culture routinely showed ~10% plaque efficiency in similar assays.

Western blotting. Western blots were performed with infected mouse sera (6 to 7 weeks p.i.; 1:200 dilution) and recombinant SAG1 and SRS9 proteins produced by the baculovirus system (11). Recombinant proteins were boiled but not reduced, and 20 μg was loaded onto one 7-cm-wide well in a 12% sodium dodecyl sulfate –polyacrylamide gel. After protein transfer, a nitrocellulose membrane was blocked in Tris-buffered saline (25 mM Tris base, 140 mM NaCl,

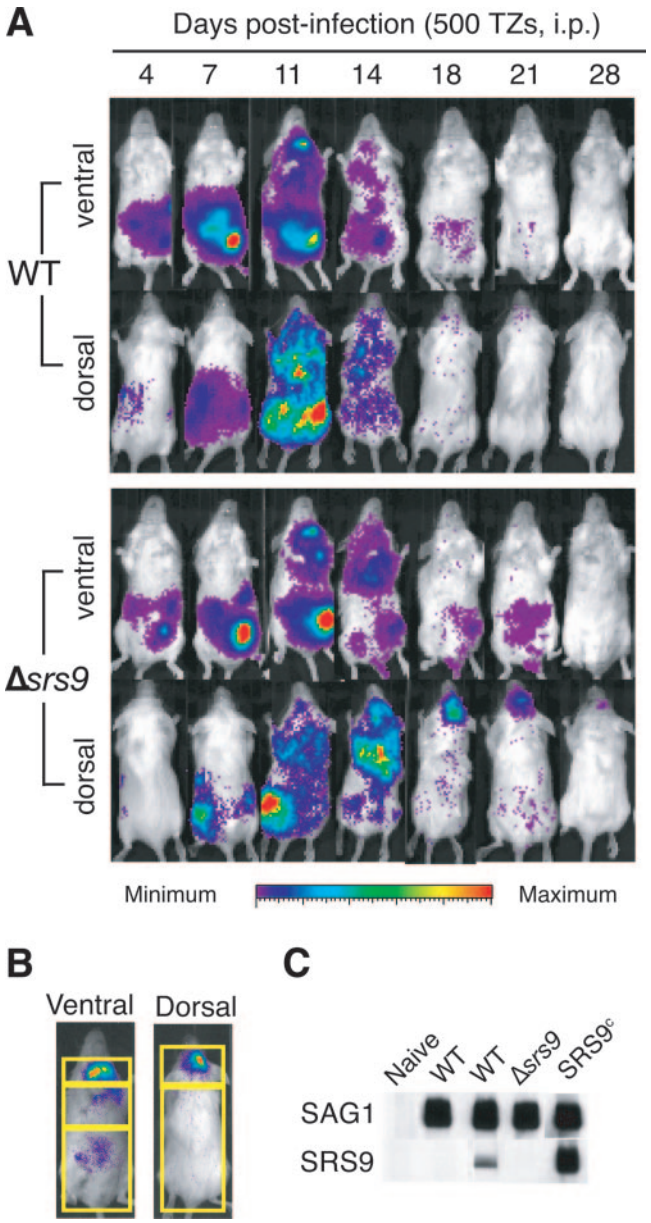

FIG. 2. Growth, dissemination, and clearance of WT and Δ*srs9* parasites in BALB/c mice infected i.p. with tachyzoites. (A) Eight-week-old BALB/c females were infected i.p. with 500 tachyzoites (TZs) of the WT or Δ*srs9* strain, and BLI was performed at the indicated days after infection. Data for one representative mouse per strain are shown. BLI was done ventrally and then dorsally, with 5 min for each side. The amount of photon flux detected in individual pixels is displayed as pseudocolor images: red represents the most intense light emission (flux greater than 10^6 and 10^5 photons/s/cm^2/steradian (sr) in ventral and dorsal images, respectively), and purple represents the weakest signal just above the background luminescence set to 6,000 photons/s/cm^2/sr. (B) Regions of interest used to quantify photon flux in infected mice summarized in Table 1. Three regions assessed in ventral images are the neck area (includes cervical lymph nodes), chest area (includes the heart and lungs), and abdominal area (includes the liver, spleen, and intestine). Total ventral signal was defined as the sum of signals in these three areas. Brain signal was determined in dorsal images (top rectangle). The total dorsal signal was defined as the sum of signals in the two rectangles shown. (C) Western blots with chronic infection sera (6 weeks p.i.) obtained from BALB/c mice infected i.p. with the indicated parasite strains. Each nitrocellulose membrane strip contains 1 μg of boiled, nonreduced recombinant SAG1 (30 kDa) or recombinant SRS9 (37 kDa). All sera were used at 1:200 dilutions. The SRS9^c strain expressing SRS9 in both tachyzoite and bradyzoite stages (11) was used as a positive control.

2.7 mM KCl) containing 5% nonfat dry milk and cut into 20 vertical strips (thus, ~1 μg protein per strip). Strips were incubated with individual mouse sera followed by peroxidase-conjugated goat anti-mouse IgG. Detection was by SuperSignal chemiluminescence reagents (Pierce Biotechnology, IL).

Statistics. Student's *t* test was performed to compare parasite loads in different experimental groups. Fisher's exact test was performed to compare the difference in the frequencies of reactivation in mice chronically infected with the WT and Δ*srs9* strains.

RESULTS

Generation of a bioluminescent Δ*srs9 Toxoplasma* strain. SRS9 is one of the most abundantly expressed SRS antigens specific to the bradyzoite stage and is a member of the SRS9 subfamily consisting of six closely related genes and one pseudogene (~50% identical at the amino acid level) (http://www.toxodb.org/toxo-release4-0/home.jsp) that are positioned tandemly on chromosome IV (Fig. 1B). The *Toxoplasma* PruΔ*hpt* strain that had been engineered to constitutively express GFP and FLUC was used to derive the Δ*srs9* parasite that lacks the entire protein-coding region by deletional mutagenesis (see Materials and Methods). After selection for clones stably expressing HPT from the knockout plasmid construct, the Δ*srs9* and WT parasites that resulted from a heterologous insertion of the construct were identified by PCR with genomic DNA (data not shown). The lack of SRS9 protein expression by the Δ*srs9* bradyzoites was confirmed by immunofluorescence assays (Fig. 1C). For animal studies, we chose WT and Δ*srs9* strains that showed similar GFP expression levels in flow cytometric analysis (data not shown) and similar FLUC activities in BLI analysis (Fig. 1D).

In intraperitoneal infection with tachyzoites, the lack of SRS9 does not alter the rates of parasite growth and dissemination or tissue tropism during an acute infection but results in reduced cyst loads persisting in the brain. To examine if the lack of SRS9 causes any changes in growth rate and tissue tropism of the parasite, we first performed i.p. infection of mice, rather than oral infection, to obtain quantitatively consistent results. BLI was performed on BALB/c females infected i.p. with 500 tachyzoites of the WT or Δ*srs9* strain throughout the course of acute and chronic infection, and representative results are shown in Fig. 2A. Photon flux produced by the parasites was quantified in different regions of the body as defined in Fig. 2B, and the results of a representative experiment are summarized in Table 1. For the most part, the WT and Δ*srs9* strains showed similar rates of expansion in all regions examined, similar dissemination kinetics up to 14 days of an acute infection, and essentially identical tissue tropisms (Fig. 2A and Table 1). The only notable difference was in the chest area at 5 days p.i., where the Δ*srs9* strain produced higher photon flux than the WT strain. It is worth noting that the lungs are the major tissue in which conversion to bradyzoites can be detected by BLI during an acute infection (J. Saeij, unpublished results).

Dramatic differences were observed between 2 weeks p.i.

TABLE 1. Quantitation of parasite loads in BALB/c mice infected i.p. with WT or Δ*srs9* tachyzoites

Strain and area of infection	Parasite load on day[a]:							
	0	5	9	14	18	22	28	35
Total ventral								
WT	363 ± 28	7,813 ± 5,665	23,813 ± 27,162	1,518 ± 764	**543 ± 116**	438 ± 57	417 ± 71	347 ± 214
Δ*srs9*	350 ± 32	7,623 ± 2,450	20,598 ± 17,482	958 ± 401	**881 ± 262**	476 ± 97	493 ± 47	436 ± 140
Neck								
WT	48 ± 5	60 ± 7	254 ± 110	110 ± 23	51 ± 7	47 ± 11	46 ± 10	51 ± 7
Δ*srs9*	50 ± 3	55 ± 8	296 ± 85	85 ± 24	66 ± 15	40 ± 9	48 ± 5	53 ± 9
Chest								
WT	92 ± 5	**164 ± 14**	402 ± 296	237 ± 99	105 ± 16	99 ± 8	89 ± 3	90 ± 7
Δ*srs9*	93 ± 4	**205 ± 33**	435 ± 102	192 ± 96	141 ± 29	98 ± 11	87 ± 5	89 ± 4
Abdomen								
WT	262 ± 33	8,560 ± 4,160	23,254 ± 26,717	1,160 ± 807	**364 ± 79**	304 ± 56	264 ± 38	250 ± 73
Δ*srs9*	279 ± 33	7,350 ± 2,413	19,940 ± 17,354	719 ± 356	**658 ± 184**	333 ± 84	328 ± 39	281 ± 106
Total dorsal								
WT	296 ± 16	ND	ND	601 ± 253	**343 ± 50**	**354 ± 36**	293 ± 24	294 ± 40
Δ*srs9*	298 ± 15	ND	ND	639 ± 130	**740 ± 115**	**438 ± 20**	281 ± 11	297 ± 23
Brain								
WT	68 ± 8	ND	ND	178 ± 53	**72 ± 12**	67 ± 7	73 ± 9	74 ± 4
Δ*srs9*	70 ± 7	ND	ND	128 ± 50	**123 ± 36**	88 ± 21	74 ± 4	72 ± 5

[a] Parasite loads are presented as photon flux detected by BLI in the regions of interest defined in Fig. 2B. Four mice per group were infected with the WT or Δ*srs9* strain (500 tachyzoites i.p.). Mean levels of flux (10^3 photons/s/cm^2/sr) ± standard deviations are shown. Notable differences are indicated in boldface and include the chest signals on day 5 ($P = 0.07$); total ventral signals ($P = 0.06$), abdominal signals ($P = 0.03$), total dorsal signals ($P = 0.004$), and brain signals ($P = 0.04$) on day 18; and total dorsal signals ($P = 0.01$) on day 22. ND, not determined, as brain signals do not appear until >10 days after infection.

and 3 weeks p.i., at which time, infection is considered to be in a chronic phase. After 18 days p.i, WT parasites are cleared from most of the body and it is unusual to detect parasite photon flux in any regions after 21 days of infection (Fig. 2A and Table 1). In contrast, Δ*srs9* parasites showed substantial photon flux at day 18 and 21 days p.i. in the abdominal area, as well as in the brain and broadly across the entire back area (i.e., total dorsal signal), indicating a delayed clearance of an acute infection (Fig. 2A and Table 1). At 6 weeks p.i., mice infected i.p. with WT tachyzoites showed no or a barely detectable serum IgG (Fig. 2C) or splenic T-cell response to SRS9 (11).

Cysts containing bradyzoites are known to rupture during a chronic infection of the brain, and when this occurs, SRS antigens expressed at the surface of bradyzoites may play a role in facilitating the invasion of new host cells and maintaining parasite persistence. To examine if SRS9 plays a role in this regard, we assessed in vitro if the lack of SRS9 expression impairs the parasite's ability to invade host cells. In plaque assays using human foreskin fibroblasts (see Materials and Methods), brain homogenates containing the equivalent of one cyst produced 103 ± 27 and 126 ± 5 plaques for the WT and Δ*srs9* strains, respectively (cyst sizes were not significantly different between WT and Δ*srs9*; see below). Far lower but similar numbers of plaques were formed when primary rat astrocytes were used: 4 ± 2 and 5 ± 2 plaques per cyst for the WT and Δ*srs9* strains, respectively. More than 90% of all WT and Δ*srs9* plaques were formed by bradyzoites, as judged by the surface expression of SAG2X and SAG2Y specific to the bradyzoite stage (data not shown).

Despite the lack of differences in invasion ability in vitro, Δ*srs9* exhibited a clearly different phenotype in the brain of chronically infected mice. We assessed brain cyst loads in chronically infected CBA/J mice in which brain cyst counts are 20- to 50-fold higher than in BALB/c mice (11) and thus allow more accurate assessment of cyst loads. As in BALB/c mice, WT and Δ*srs9* strains showed comparable expansion and dissemination during an acute infection in CBA/J mice infected i.p. with 500 tachyzoites (data not shown). Mortalities were similar in that two of eight WT-infected CBA/J mice and one of eight Δ*srs9* strain-infected mice died by 26 days after i.p. infection. In two separate experiments, WT and Δ*srs9* brain cyst numbers were comparable at the early phase of a chronic infection (3 and 4 weeks p.i. in Fig. 3A). However, at 6 and 11 weeks p.i., Δ*srs9* cyst loads were significantly lower than those of the WT (Fig. 3A). The decrease in Δ*srs9* cyst loads was not due to a growth defect in the bradyzoite stage: the size of Δ*srs9* brain cysts was comparable to that of WT cysts, suggesting a similar growth rate between WT and Δ*srs9* bradyzoites (Fig. 3B).

The WT and Δ*srs9* strains show comparable oral infectivities, but unlike the WT strain, the Δ*srs9* strain reactivates early in the intestine when chronically infected mice become immunosuppressed. It has been speculated that SRS antigens specific to the bradyzoite stage may serve as cell-type-specific adhesion molecules during the invasion of the intestinal epithelium upon oral infection with tissue cysts. To examine if SRS9 plays such a role, we infected BALB/c females orally by feeding brain homogenates containing 300 WT or Δ*srs9* cysts placed on top of a small piece of normal diet and monitored infection over time by BLI. We chose feeding over oral gavage because the latter procedure gave inconsistent courses of in-

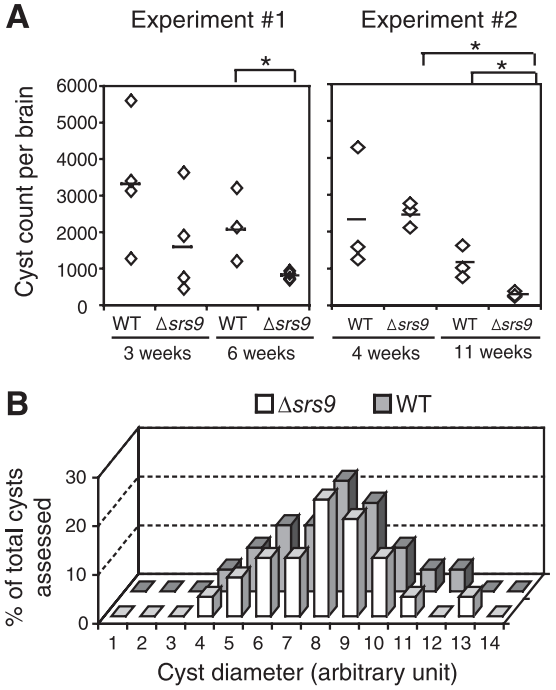

FIG. 3. Comparison of brain cyst loads in CBA/J mice infected i.p. with WT or Δ*srs9* parasites. (A) Brain cyst counts in chronically infected CBA/J females after i.p. infection with 500 tachyzoites of the WT or Δ*srs9* strain. Bars indicate average cyst counts of given groups, and asterisks indicate a statistically significant ($P < 0.05$) reduction between two groups. (B) Cyst diameter was measured in photographed hematoxylin- and eosin-stained brain sections from chronically infected CBA/J mice (6 weeks p.i.) and is presented in arbitrary units. The numbers of cysts assessed were 22 for the WT strain and 25 for the Δ*srs9* strain.

fection with occasional initial foci of parasite replication in the neck region, perhaps, due to esophageal damage during gavage (J. Boyle, unpublished results).

As expected due to the nature of the procedure, oral infection by feeding showed large individual variations in the timing and degree of parasite expansion (Fig. 4A and B) and did not allow accurate quantitative comparison between the WT and Δ*srs9* strains. Nonetheless, it was clear that the Δ*srs9* strain was not severely impaired in its oral infectivity: with both WT and Δ*srs9* strains, parasites were first detected 5 to 7 days p.i. in a Peyer's patch in the duodenum and were soon disseminated to various distant tissues (Fig. 4A and B). By 9 days p.i., both WT (Fig. 4C) and Δ*srs9* parasites (data not shown) were detectable in multiple Peyer's patches along the small intestine (1) and in mesenteric lymph nodes, as well as in the spleen, liver, lungs, and cervical lymph nodes. As with i.p. infection, the Δ*srs9* strain showed delayed clearance from the brain between 15 and 21 days p.i. (Fig. 4B).

At 6 weeks p.i., all mice orally infected with WT or Δ*srs9* cysts showed equally strong serum IgG responses to tachyzoite-specific SRS antigen SAG1, as expected (Fig. 4D). Also, perhaps as expected from the large number of cysts given, all mice infected with 300 WT cysts had a readily detectable serum IgG response to recombinant SRS9 protein (Fig. 4D), and the titer appeared to correlate with the size of parasite expansion in the intestinal tissue (see Fig. 4A for BLI data for matching mice).

As a means of examining the parasite's ability to persist and the host's ability to control parasite replication, we reactivated chronically infected mice 8 weeks after the oral infection by adding the immunosuppressant DXM to drinking water (30 mg/liter). Out of 10 mice orally infected with the WT strain, 5 mice showed a strong parasite replication in multiple tissues after 14 to 15 days of DXM treatment (data for 3 of them are presented in Fig. 4E); 1 mouse survived through 16 days of DXM treatment, showing only minor parasite replication in the liver on the 9th and 10th days of drug treatment (data not shown); and 4 mice showed no or barely detectable parasite replication at multiple sites, mostly lymph nodes, but died after 14 days of DXM treatment (data not shown).

In contrast, three of seven mice (43%) infected with the Δ*srs9* strain showed an early, intense reactivation in the intestinal tissue between 8 and 9 days after DXM treatment, before reactivation could be detected in other tissues (see ventral images in Fig. 4F). As described above, none of the 10 WT-infected mice (0%) showed the kind of early reactivation seen in the intestinal tissue of Δ*srs9* strain-infected mice (Fisher's exact test value of $P = 0.052$ at the 95% confidence level). Another distinct site of early Δ*srs9* reactivation was a lymph node in the center of the back of a mouse (see dorsal images in Fig. 4F). Three other mice in this group showed a minor reactivation limited to one or two lymphoid structures in the abdominal area between 10 and 16 days of DXM treatment (data not shown). One of seven mice infected with the Δ*srs9* strain reactivated similarly to WT and showed a strong parasite replication in multiple tissues after 14 days of DXM treatment (data not shown).

DISCUSSION

The surface of *Toxoplasma gondii* is dominated by closely related surface proteins belonging to the SRS superfamily. SRS antigens expressed at different developmental stages may have evolved to allow parasite binding to cell-specific ligands of the host cell types relevant to the given stage. For example, bradyzoite-specific SRS antigens may be particularly important in interacting with intestinal epithelial cells following an oral infection with tissue cysts and/or as-yet-unidentified host cells in the brain, as well as activating and recruiting an adaptive immune response to these tissues. In this study, we chose SRS9 as a model antigen to explore these questions, utilizing bioluminescent WT and Δ*srs9* strains.

In mice infected i.p. with tachyzoites, early growth and dissemination characteristics and tissue tropism were indistinguishable between WT and Δ*srs9* parasites. The only difference was higher parasite loads in Δ*srs9* strain infection than in WT infection in the lungs at 5 days p.i., as well as in the abdomen and brain at 18 to 21 days p.i.. Bradyzoites can be detected in the lungs and brains of acutely infected mice, and it is possible that WT parasites induce SRS9-specific immune responses that, although barely detectable by conventional assays, can still contribute to bradyzoite clearance during an acute infection of tissues such as the abdomen, lungs, and brain. Mice infected with the Δ*srs9* strain lack such immune responses, which may be why Δ*srs9* parasites appear to be cleared more slowly from the tissues mentioned above.

Notably, the Δ*srs9* strain resulted in significantly lower brain

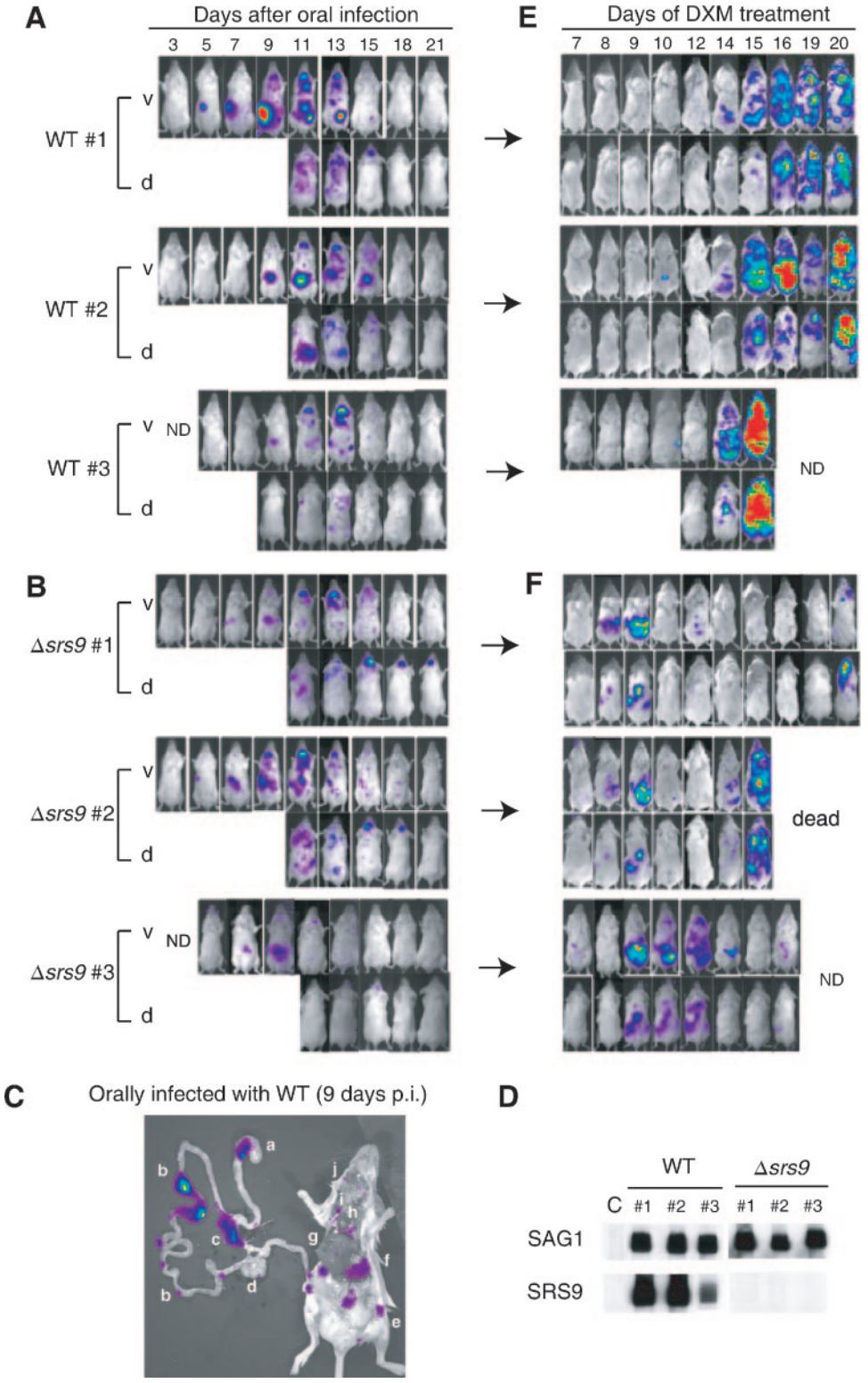

FIG. 4. BLI of BALB/c mice orally infected with WT and Δ*srs9* cysts and reactivated during a chronic infection. BALB/c females were infected with the WT strain (A) or Δ*srs9* strain (B) orally by feeding them brain homogenates containing 300 cysts. The course of acute infection revealed by BLI is shown for three mice per strain. (C) Ex vivo imaging of the gastrointestinal tract and other tissues. At 9 days p.i., mice orally infected with 300 WT cysts were injected with luciferin and sacrificed before BLI. The lowercase letters indicate the following: a, stomach; b, Peyer's patches; c, mesenteric lymph nodes; d, cecum; e, inguinal lymph node; f, spleen; g, liver; h, heart; i, lung; and j, cervical lymph node. (D) Western blots with sera (6 weeks p.i.) obtained from BALB/c mice with chronic infection shown in panels A and B. Each nitrocellulose membrane strip contains 1 μg of boiled, nonreduced recombinant SAG1 (30 kDa) or recombinant SRS9 (37 kDa) protein. Uninfected mouse serum was used as a negative control ("C"). All sera were used at 1:200 dilutions. (E and F) Mice shown in panels A and B began to receive DXM (30 mg/liter of drinking water) at 8 weeks p.i. BLI was performed on the indicated days of drug treatment. Color scales for panels A, B, C, E, and F are the same as those shown in Fig. 2A. ND, not done; v, ventral image; d, dorsal image.

cyst loads than the WT strain at the late phase of a chronic infection, contrary to what would have been expected if anti-SRS9 response would be effective in the chronically infected brain. Thus, it seems likely that Δ*srs9* parasites are impaired in their ability to infect new host cells and maintain persistent infection of the brain. WT and Δ*srs9* strains did not show significant differences in the in vitro invasion assays we performed with human fibroblasts and rat astrocytes. Clearly, however, the true target cells in the mouse brain preferentially infected by *Toxoplasma* are yet to be identified and investigated in invasion assays. Nonetheless, it is interesting to note that the lack of SRS9 expression compromised the parasite's ability to persist in the brain when other SRS antigens specific to the bradyzoite stage, especially the members of the SRS9 subfamily (e.g., the gene immediately downstream of SRS9 that has ESTs in the bradyzoite stage), may be functionally redundant to SRS9. It is not known if and how the absence of SRS9 changes the surface structure and expression patterns of the remaining members of the SRS9 subfamily. To better understand the functions of SRS9 and other bradyzoite-specific relatives, it will be necessary to examine whether, and at what stage, the members of the SRS9 subfamily are expressed by WT and Δ*srs9* strains and what effect a deletion of the entire region containing the *SRS9* locus has on the pathogenesis.

In contrast to the reduced ability to maintain infection in the brain, Δ*srs9* parasites showed a similar oral infectivity to WT parasites and at least initially disseminated to and replicated in the same tissues as WT parasites. If all oral infection occurs via the invasion of the intestinal epithelium, our data would suggest that SRS9 is not single-handedly responsible for parasite attachment to and invasion of the intestinal epithelium. It has been shown that dendritic cells present in the lamina propria can directly sample antigens passing through the lumen of the small intestine by extending their dendrites across the epithelial barrier and into the lumen (14, 17). This phenomenon is yet to be investigated in oral infection with *Toxoplasma*, but infection of such cells could be an important mechanism by which parasites rapidly disseminate systematically. To fully appreciate the role of SRS9 as a cell adhesion molecule, it would be important to examine if WT and Δ*srs9* parasites infect intestinal epithelial cells and enter dendritic cells with equal levels of efficiency.

Although many unanswered questions remain about the role of SRS9 as a cell adhesion molecule, its immunological role has become strikingly clear. Previously, we have demonstrated that SRS9 protein, if given with an appropriate adjuvant or if constitutively expressed at both tachyzoite and bradyzoite stages, is capable of activating serum IgG and gamma interferon-producing T-cell responses associated with a substantial reduction in the number of persisting parasites (11). In the present study, we have found that SRS9 may be an important target of the host immune response in the intestine in mice that consumed a high dose of bradyzoite cysts. In mice chronically infected with the WT strain showing strong serum IgG responses to SRS9, it usually took 14 days of DXM treatment to immunosuppress the animals before active parasite replication could be seen in the abdominal area—and all over the body soon thereafter. In contrast, Δ*srs9* parasites showed an early, intense reactivation in the intestinal tissue after only 8 to 9 days of DXM treatment. This suggests that the local environment in the intestine of a Δ*srs9*-infected mouse lacks a protective component, presumably an SRS9-specific immune response, and, therefore, allows parasites to grow. Thus, it seems that if a robust parasite (bradyzoite) replication occurs in the intestine following ingestion of numerous cysts, SRS9 can elicit a protective immune response that stays locally in the gut for a long time. However, ingestion of 300 cysts as we have used in this study is an unlikely event in nature, and naturally infected people and animals, for the most part, may lack detectable immune responses against SRS9 and other bradyzoite antigens.

The early reactivation of Δ*srs9* parasites in the intestine of immunosuppressed mice raises the possibility that the intestine may be one of the major sites of parasite persistence following an oral infection, which may be why reactivation is first detected there. Due to the lack of a protective (SRS9 specific) immune response in the intestinal tissue, more Δ*srs9* parasites than WT parasites may have been allowed to persist in the intestinal tissues, probably in Peyer's patches and mesenteric lymph nodes where parasite replication was observed during an acute infection. Soon after the initiation of DXM treatment, Δ*srs9* parasites, unlike WT parasites, would be allowed to expand in the intestinal tissue. By using parasite GFP and FLUC activity as readouts, we were unable to detect parasites in the Peyer's patches, mesenteric and other lymph nodes, spleen, liver, or lungs of chronically infected mice (8 weeks p.i.; data not shown), but it is quite possible that *Toxoplasma* persists in these tissues at a level below detection. The brain, which is widely perceived to be the major site of parasite persistence, was the only tissue in which we could detect parasites (30 to 100 cysts per BALB/c mouse brain in i.p. infection with 500 tachyzoites) during a chronic infection. Upon DXM treatment, parasites may reactivate in the brain and disseminate to multiple distant tissues. Since most tissues should have a strong immune response targeting tachyzoite antigens (which are identical in the WT and Δ*srs9* strains), levels of WT and Δ*srs9* parasite replication would be controlled equally well until the host becomes severely immunosuppressed after 2 weeks of DXM treatment. The intestinal tissue may be unique in that a large amount of bradyzoite antigens may have been presented to the immune system and may contain immune responses directed to bradyzoites, in addition to tachyzoites. The Δ*srs9* parasites that have migrated from the brain may be allowed to expand in the intestine due to the lack of an immune response targeting SRS9.

If the early reactivation of Δ*srs9* parasites seen in the intestinal tissue is indeed due to the lack of a protective, anti-SRS9 response, this implies that parasites initially replicate as bradyzoites when DXM treatment is initiated. Utilizing stage-specific promoters to drive the expression of FLUC in WT and Δ*srs9* strains will produce useful information regarding in which tissues and by what mechanisms *Toxoplasma* stage conversion occurs and improve our understanding of the immunological role of bradyzoite-specific SRS antigens.

ACKNOWLEDGMENTS

We thank Upi Singh (Stanford University) for suggesting that in vitro bradyzoites, rather than tachyzoites, be used in our attempt to achieve a double-homologous recombination at the *SRS9* locus, which

clearly helped create the *SRS9* knockout strain. We thank Chris Contag and Timothy Dolye at the Small Animal Imaging Facility (Stanford University) for their technical assistance and helpful discussion about bioluminescence imaging and J. Saeji and J. Boyle for communicating unpublished results.

This research was supported by National Institutes of Health grants AI41014 and AI21423 to J.C.B. and, in part, through grant R24CA92862 from the National Cancer Institute's Small Animal Imaging Resource Program.

REFERENCES

1. **Beilhack, A., S. Schulz, J. Baker, G. F. Beilhack, C. B. Wieland, E. I. Herman, E. M. Baker, Y. A. Cao, C. H. Contag, and R. S. Negrin.** 2005. In vivo analyses of early events in acute graft-versus-host disease reveal sequential infiltration of T-cell subsets. Blood **106:**1113–1122.
2. **Bessieres, M. H., S. Le Breton, and J. P. Seguela.** 1992. Analysis by immunoblotting of *Toxoplasma gondii* exo-antigens and comparison with somatic antigens. Parasitol. Res. **78:**222–228.
3. **Brenier-Pinchart, M. P., I. Villena, C. Mercier, F. Durand, J. Simon, M. F. Cesbron-Delauw, and H. Pelloux.** 2006. The *Toxoplasma* surface protein SAG1 triggers efficient in vitro secretion of chemokine ligand 2 (CCL2) from human fibroblasts. Microbes Infect. **8:**254–261.
4. **Djurkovic-Djakovic, O., and V. Milenkovic.** 2001. Murine model of drug-induced reactivation of *Toxoplasma gondii*. Acta Protozool. **40:**99–106.
5. **Donald, R. G., and D. S. Roos.** 1998. Gene knock-outs and allelic replacements in *Toxoplasma gondii*: HXGPRT as a selectable marker for hit-and-run mutagenesis. Mol. Biochem. Parasitol. **91:**295–305.
6. **Dzierszinski, F., M. Mortuaire, M. F. Cesbron-Delauw, and S. Tomavo.** 2000. Targeted disruption of the glycosylphosphatidylinositol-anchored surface antigen SAG3 gene in *Toxoplasma gondii* decreases host cell adhesion and drastically reduces virulence in mice. Mol. Microbiol. **37:**574–582.
7. **He, X.-L., M. E. Grigg, J. C. Boothroyd, and K. C. Garcia.** 2002. Structure of the immunodominant surface antigen from the *Toxoplasma gondii* SRS superfamily. Nat. Struct. Biol. **9:**606–611.
8. **Hitziger, N., I. Dellacasa, B. Albiger, and A. Barragan.** 2005. Dissemination of *Toxoplasma gondii* to immunoprivileged organs and role of Toll/interleukin-1 receptor signaling for host resistance assessed by in vivo bioluminescence imaging. Cell. Microbiol. **7:**837–848.
9. **Jacquet, A., L. Coulon, J. De Neve, V. Daminet, M. Haumont, L. Garcia, A. Bollen, M. Jurado, and R. Biemans.** 2001. The surface antigen SAG3 mediates the attachment of *Toxoplasma gondii* to cell-surface proteoglycans. Mol. Biochem. Parasitol. **116:**35–44.
10. **Jung, C., C. Y. Lee, and M. E. Grigg.** 2004. The SRS superfamily of Toxoplasma surface proteins. Int. J. Parasitol. **34:**285–296.
11. **Kim, S. K., and J. C. Boothroyd.** 2005. Stage-specific expression of surface antigens by *Toxoplasma gondii* as a mechanism to facilitate parasite persistence. J. Immunol. **174:**8038–8048.
12. **Mercier, C., S. Lefebvre-Van Hende, G. E. Garber, L. Lecordier, A. Capron, and M. F. Cesbron-Delauw.** 1996. Common cis-acting elements critical for the expression of several genes of *Toxoplasma gondii*. Mol. Microbiol. **21:**421–428.
13. **Mineo, J. R., and L. H. Kasper.** 1994. Attachment of *Toxoplasma gondii* to host cells involves major surface protein, SAG-1 (P30). Exp. Parasitol. **79:**11–20.
14. **Niess, J. H., S. Brand, X. Gu, L. Landsman, S. Jung, B. A. McCormick, J. M. Vyas, M. Boes, H. L. Ploegh, J. G. Fox, D. R. Littman, and H. C. Reinecker.** 2005. CX3CR1-mediated dendritic cell access to the intestinal lumen and bacterial clearance. Science **307:**254–258.
15. **Partanen, P., H. J. Turunen, R. T. A. Paasivuo, and P. O. Leinikki.** 1984. Immunoblot analysis of *Toxoplasma gondii* antigens by human immunoglobulins G, M, and A antibodies at different stages of infection. J. Clin. Microbiol. **20:**133–135.
16. **Rachinel, N., D. Buzoni-Gatel, C. Dutta, F. J. Mennechet, S. Luangsay, L. A. Minns, M. E. Grigg, S. Tomavo, J. C. Boothroyd, and L. H. Kasper.** 2004. The induction of acute ileitis by a single microbial antigen of *Toxoplasma gondii*. J. Immunol. **173:**2725–2735.
17. **Rescigno, M., M. Urbano, B. Valzasina, M. Francolini, G. Rotta, R. Bonasio, F. Granucci, J. P. Kraehenbuhl, and P. Ricciardi-Castagnoli.** 2001. Dendritic cells express tight junction proteins and penetrate gut epithelial monolayers to sample bacteria. Nat. Immunol. **2:**361–367.
18. **Robinson, S. A., J. E. Smith, and P. A. Millner.** 2004. *Toxoplasma gondii* major surface antigen (SAG1): in vitro analysis of host cell binding. Parasitology **128:**391–396.
19. **Saeij, J. P. J., J. P. Boyle, M. E. Grigg, G. Arrizabalaga, and J. C. Boothroyd.** 2005. Bioluminescence imaging of *Toxoplasma gondii* infection in living mice reveals dramatic differences between strains. Infect. Immun. **73:**695–702.
20. **Soldati, D., and J. C. Boothroyd.** 1993. Transient transfection and expression in the obligate intracellular parasite *Toxoplasma gondii*. Science **260:**349–352.
21. **Tenter, A. M., A. R. Heckeroth, and L. M. Weiss.** 2000. *Toxoplasma gondii*: from animals to humans. Int. J. Parasitol. **30:**1217–1258.
22. **Tomavo, S.** 1996. The major surface proteins of *Toxoplasma gondii*: structures and functions. Curr. Top. Microbiol. Immunol. **219:**45–54.

Editor: W. A. Petri, Jr.